

Article

# Biomechanical and machine learning approaches to automating the identification of musical styles and emotions through human motion analysis

Yuan Ding

Nantong Normal College, Nantong 226010, China; YuanDing19@outlook.com

## CITATION

Ding Y. Biomechanical and machine learning approaches to automating the identification of musical styles and emotions through human motion analysis. *Molecular & Cellular Biomechanics*. 2024; 21(2): 397. <https://doi.org/10.62617/mcb.v21i2.397>

## ARTICLE INFO

Received: 20 September 2024  
Accepted: 8 October 2024  
Available online: 6 November 2024

## COPYRIGHT



Copyright © 2024 by author(s).  
*Molecular & Cellular Biomechanics* is published by Sin-Chn Scientific Press Pte. Ltd. This work is licensed under the Creative Commons Attribution (CC BY) license. <https://creativecommons.org/licenses/by/4.0/>

**Abstract:** This study explores the intricate relationship between biomechanical movements and musical expression, focusing on the identification of musical styles and emotions. Violin performance is characterized by complex interactions between physical actions—such as bowing techniques, finger placements, and posture—and the resulting acoustic output. Recent advances in motion capture technology and sound analysis have enabled a more objective examination of these processes. However, the current literature frequently addresses biomechanics and acoustic features in isolation, lacking an integrated understanding of how physical movements translate into specific musical expressions. Machine Learning (ML), particularly Long Short-Term Memory (LSTM) networks, provides a promising avenue for bridging this gap. LSTM models are adept at capturing temporal dependencies in sequential data, making them suitable for analyzing the dynamic nature of violin performance. In this work, they have proposed a comprehensive model that combines biomechanical analysis with Mel-spectrogram-based LSTM modeling to automate the identification of musical styles and emotions in violin performances. Using motion capture systems, Inertial Measurement Units (IMUs), and high-fidelity audio recordings, we collected synchronized biomechanical and acoustic data from violinists performing various musical excerpts. The LSTM model was trained on this dataset to learn the intricate connections between physical movements and the acoustic features of each performance. Key findings from the study demonstrate the effectiveness of this integrated approach. The LSTM model achieved a validation accuracy of 92.5% in classifying musical styles and emotions, with precision, recall, and F1-score reaching 94.3%, 92.6%, and 93.4%, respectively, by the 100th epoch. The analysis also revealed strong correlations between specific biomechanical parameters, such as shoulder joint angle and bowing velocity, and acoustic features, like sound intensity and vibrato amplitude.

**Keywords:** biomechanical movements; machine learning; musical styles; emotions; physical movements; joint angle and bowing velocity; motion capture

## 1. Introduction

Music performance, particularly in instruments like the violin, is a complex interplay of Physical Movements (PM) and Emotional Expression (EE) [1,2]. Violinists convey a wide range of emotions and musical styles through precise control of their movements, such as bowing techniques, finger placements, and body posture [3,4]. The study of these movements and their impact on musical output has been a subject of interest in fields like musicology, biomechanics, and music cognition [5]. Traditionally, research in this area has focused on qualitative analyses and subjective interpretations to understand how musicians produce expressive performances [6–8]. However, these methods frequently lack the precision to fully capture the intricate biomechanical processes involved in violin playing [9].

In recent years, technological advancements have enabled more detailed investigations into the biomechanics of musical performance [10–12]. Current studies employ motion capture systems and Inertial Measurement Units (IMUs) to record the PM of musicians, offering a more objective view of how different playing techniques contribute to ME [13,14]. Similarly, acoustic analysis, mainly through the use of Mel-spectrograms, has provided insights into the audio features that correspond with emotional and stylistic variations in music [15,16]. Despite these advances, the relationship between Biomechanical Movements (BM) and acoustic features remains underexplored in an integrated and automated manner [17]. Most existing research approaches this relationship through isolated analyses, frequently lacking a unified framework that comprehensively connects performance’s physical and acoustic aspects [18]. This limitation makes it challenging to understand how specific movements influence the perceived musical output.

Machine Learning (ML), particularly Neural Network (NN) models like Long Short-Term Memory (LSTM), offers a promising solution to this problem [19]. LSTM networks can model complex temporal dependencies in sequential data, making them ideal for analyzing the dynamic nature of music performance [20]. They can capture long-term relationships between a violinist’s movements and the resulting sound, facilitating identifying patterns corresponding to various musical styles and emotional contexts. Unlike traditional analysis methods, ML can process large, multi-dimensional datasets, allowing for a more nuanced and automated analysis of the interplay between biomechanics and music [21–25]. This provides an opportunity to move beyond subjective evaluation and uncover the underlying mechanisms of ME with greater accuracy and detail [26–30].

The proposed work aims to address the limitations of current research by developing a framework that integrates biomechanical analysis with a Mel-spectrogram-based LSTM model to automate the identification of musical styles and emotions in violin performances. The proposed work explores the intricate relationship between BM and sound features in violin performances to automate the identification of musical styles and emotions. By combining Motion Capture (MC) technology, IMUs, and audio recording, detailed data on joint angles, forces, and sound characteristics are collected from violinists performing a variety of musical excerpts. Mel-spectrograms are used to extract time-frequency features from the audio, providing a nuanced representation of the music’s expressive elements. The study leverages a Mel-spectrogram-based LSTM model to analyze this multi-dimensional dataset. The LSTM, trained on synchronized biomechanical and acoustic data, learns to recognize patterns corresponding to different musical styles and emotional contexts. The work not only enhances the understanding of how PM contributes to ME but also demonstrates the potential of ML in automating the analysis of performance characteristics in music.

The paper is organized as follows: Section 2 presents the methodology, Section 3 presents the methodology, Section 4 presents the analysis, and Section 5 concludes the paper.

## **2. Methodology**

### **2.1. Participants**

The study involved 17 violinists, comprising 11 Males and 6 Females, aged between 20 and 35 years, with a mean age of 27.4 years. All participants were skilled violinists with varying experience levels, ensuring diverse performance styles and emotional expressions. Specifically, 10 participants were professional violinists with over five years of experience performing in various settings such as orchestras, chamber music groups, and solo performances. The remaining 7 participants were advanced amateurs with at least three years of dedicated practice and performance experience, often participating in community orchestras, ensembles, or solo recitals. This blend of professional and amateur musicians provided a rich dataset for examining the biomechanical nuances of violin playing across different levels of expertise [31,32].

Participants were selected based on their familiarity with a broad repertoire of musical styles, including classical, contemporary, and folk music. This variety ensured that their physical expressions—such as bowing techniques, posture, and body movement—could be analyzed concerning different musical genres and emotional contexts. Educational backgrounds varied, with 13 participants holding formal music education degrees, ranging from undergraduate to master's levels in violin performance. The remaining 4 participants, while not formally educated in music, had extensive training through private lessons and had performed regularly in semi-professional settings.

Each participant provided informed consent and completed a detailed questionnaire outlining their performance experience, preferred musical genres, and previous participation in biomechanical or music cognition studies. This information helped contextualize their movement patterns during the study. By focusing solely on violinists, the study aimed to explore the intricate relationship between a musician's physical motion—such as bowing dynamics, hand movements, and body posture—and the expressive qualities of their performance, thus contributing to the understanding of how musical styles and emotions are embodied in the art of violin playing.

### **2.2. Measurements**

To comprehensively analyze the biomechanical and expressive elements of violin performance, a multi-dimensional set of measurements was employed (**Table 1**), capturing various aspects of the participants' movements, posture, and the resulting musical output. Kinematic, kinetic, and acoustic parameters were the primary categories of measurements used to gain a holistic understanding of how violinists express musical styles and emotions.

- 1) Kinematic Measurements were primarily obtained through the motion capture system and IMUs. These measurements included joint angles at the shoulder, elbow, and wrist to assess the range of motion and the fluidity of bowing and fingering movements. Segmental velocities, both linear and angular, of the upper arm, forearm, and hand were also recorded to understand the speed and dynamics

of the violinists' techniques. The trajectory and angle of the bow relative to the strings were meticulously tracked, providing insights into the nuances of bowing style and technique that are essential for identifying variations in musical expression. Additionally, postural adjustments of the head, torso, and lower body were monitored to evaluate the violinists' overall posture and balance, capturing subtle shifts in body movement that might indicate emotional expression or stylistic interpretation.

- 2) Kinetic Measurements were collected using the force plate and IMUs to explore the forces and torques involved in violin performance. Ground reaction forces recorded by the force plate provided weight distribution and balance data during different performance phases, highlighting how the violinists' stance and lower body dynamics contributed to their overall expressiveness. The IMUs also offered detailed information on the forces exerted by the arms and hands, including the intensity of bowing and the pressure applied to the strings, which are crucial for creating sound and emotional tone variations.
- 3) Acoustic Measurements were captured using a high-fidelity microphone, synchronized with the MC and kinetic data. This allowed for a direct correlation between PM and the resulting sound. Acoustic parameters such as sound intensity, articulation, and vibrato were analyzed to understand how specific biomechanical actions influenced the musical output. By integrating these kinematic, kinetic, and sound measurements, the study aimed to unravel the complex interplay between a violinist's physical movements and their expressive musical performance, providing a detailed framework for understanding the embodiment of musical styles and emotions.

**Table 1.** Measurements.

Measurement type	Parameter	Description	Units
Kinematic	Joint angles	Angles at shoulder, elbow, and wrist joints.	Degrees (°)
	Segmental velocities	Linear and angular velocities of the arm segments.	Meters per second (m/s), Degrees per second (°/s)
	Bow trajectory and angle	Path and angle of the bow relative to violin strings.	Meters (m), Degrees (°)
	Postural adjustments	Movements of the head, torso, and lower body.	Meters (m), Degrees (°)
Kinetic	Ground reaction forces	Forces exerted on the ground during the performance.	Newtons (N)
	Arm and hand forces	Forces applied by arms and hands.	Newtons (N)
Acoustic	Sound intensity	The volume of the sound produced.	Decibels (dB)
	Articulation	Clarity and distinctness of musical notes.	Qualitative (Categorical)
	Vibrato characteristics	Frequency and amplitude of vibrato.	Hertz (Hz), Amplitude (mm)

### 2.3. Conceptual framework

The conceptual framework of this study (**Figure 1**) integrates biomechanics, music cognition, and ML to explore how violinists' movements are linked to musical styles and emotional expression. The framework is built on the premise that the PM involved in violin playing—such as bowing techniques, finger placements, and postural adjustments—are not merely mechanical features but are deeply intertwined

with the ME. By analyzing these movements with the resulting sound, the study aims to decode the underlying patterns that characterize different musical styles and emotional contexts.

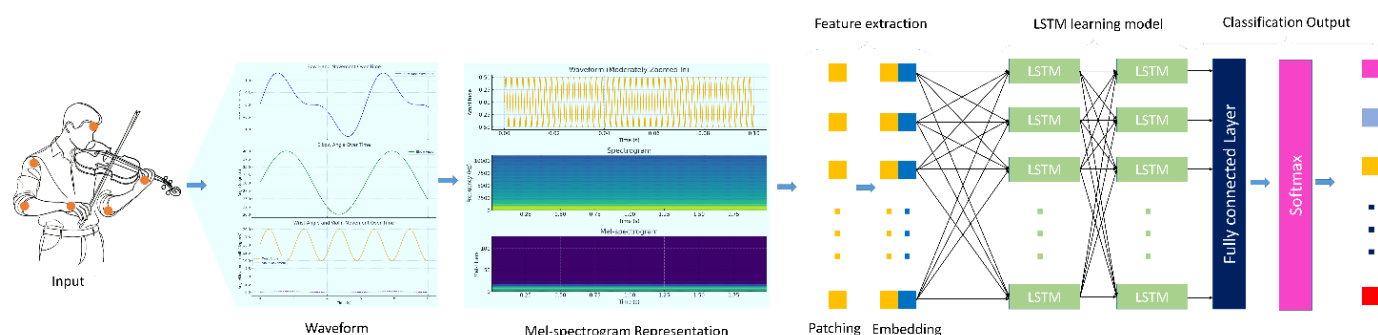


**Figure 1.** Framework of the study.

Central to this framework is the dual analysis of biomechanical data and audio output. The biomechanical feature involves capturing the violinists' movements, including joint angles, segmental velocities, and force dynamics, to understand the physical expression of their performances. The acoustic aspect focuses on the audio features of the performance, with a specific emphasis on how the energy distribution across frequencies reflects the nuances of the music being played. By combining these two aspects, the framework seeks to uncover the complex relationship between a musician's physical movements and the expressive qualities of their performance.

The ML component is then employed to automate the identification of musical styles and emotions. By processing both biomechanical and audio data, the framework leverages advanced algorithms to identify patterns and correlations within this multi-dimensional dataset. The aim is to develop a system that recognizes and categorizes ME by analyzing how violinists embody different styles and emotions through their movements. This integrated approach offers a holistic view of ME, advancing the understanding of how PM and sound interact in violin playing.

## 2.4. Data collection

Data collection was meticulously designed to capture both the BM of the violinists and the corresponding acoustic output during the performance. Participants were instructed to perform a series of musical excerpts that spanned a range of styles and emotional contexts. High-fidelity audio recordings were made of each performance, which were then processed to extract detailed acoustic features. This included capturing the music's frequency, intensity, and timbral features, contributing a nuanced view of the expressive elements in each piece.

In parallel, biomechanical data were collected using a motion capture system with 12 high-speed infrared cameras and wearable IMUs. Reflective markers were placed on key anatomical landmarks, such as the head, shoulders, elbows, and wrists, to capture the complex motions involved in violin playing. This setup enabled the precise measurement of kinematic parameters, including joint angles, segmental velocities, and bowing trajectories. The IMUs complemented this data by providing additional insights into angular velocities and forces exerted by the arms and hands. A force plate

embedded in the floor measured ground reaction forces, showing the participants' balance and weight distribution during the performance.

To ensure a comprehensive dataset, the audio and motion data were synchronized, allowing for integrated analysis of how specific movements influenced the acoustic output. Each musical excerpt was performed multiple times to capture various expressive variations. The collected data were then processed into a format suitable for ML analysis, with sequences representing temporal performance windows. This comprehensive data collection approach aimed to provide a rich foundation for examining the interplay between the biomechanical features of violin playing and the resulting musical expression, facilitating an in-depth exploration of how physical movement and sound are interconnected in conveying musical styles and emotions.

## 2.5. Mel-Spectrogram-based LSTM

The Mel-spectrogram-based LSTM was employed to analyze the temporal relationships between violinists' BM and the audio features of their performances. The model utilized Mel-spectrograms, which provide a time-frequency representation of the audio signal, combined with biomechanical data to capture patterns corresponding to different musical styles and emotions. The LSTM was chosen due to its ability to learn and model long-term dependencies in sequential data, making it ideal for understanding violin performance's dynamic and expressive nature.

- 1) Input to the LSTM: The input to the LSTM consisted of sequences of feature vectors representing biomechanical and audio data. Each input sequence  $X$  was structured as follows:

$$X = \{(x_1, m_1), (x_2, m_2), \dots, (x_T, m_T)\} \quad (1)$$

where  $x_t$  is the biomechanical feature vector at time  $t$  including joint angles, velocities, forces, and  $m_t$  is the Mel-spectrogram frame at the same time  $t$ . Mel-spectrograms were derived from the audio signal using the Short-Time Fourier Transform (STFT):

$$\text{STFT}\{x(t)\}(t, f) = \sum_{n=0}^{N-1} x[n] \times w[n-t] e^{-j2\pi f n/N} \quad (2)$$

The Mel-spectrogram  $M(t, f_{mel})$  was then calculated by mapping the frequency components onto the Mel scale:

$$M(t, f_{mel}) = \sum_k |STFT\{x(t)\}(t, f_k)|^2 \times H(f_k, f_{mel}) \quad (3)$$

where  $H(f_k, f_{mel})$  is the Mel filter bank. This transformation provided a feature-rich representation of the audio that captured the expressive elements of the musical performance.

- 2) LSTM: The model's core comprised multiple layers of LSTM units. Each LSTM unit maintained an internal state  $c_t$  and an output  $h_t$  at each time step. It used three gates-input, forget, and output gates-to regulate the flow of information:

- Input Gate  $i_t$ :

$$i_t = \sigma(W_i \times [h_{t-1}, x_t] + b_i) \quad (4)$$

- Forget Gate  $f_t$ :

$$f_t = \sigma(W_f \times [h_{t-1}, x_t] + b_f) \quad (5)$$

- Output Gate  $o_t$ :

$$o_t = \sigma(W_o \times [h_{t-1}, x_t] + b_o) \quad (6)$$

- Cell state update:

$$\tilde{c}_t = \tanh(W_c \times [h_{t-1}, x_t] + b_c) \quad (7)$$

$$c_t = f_t \cdot c_{t-1} + i_t \cdot \tilde{c}_t \quad (8)$$

- Hidden state  $h_t$ :

$$h_t = o_t \times \tanh(c_t) \quad (9)$$

Here,  $\sigma$  is the sigmoid activation function, and  $\tanh$  is the hyperbolic tangent function.  $W_i, W_f, W_o$ , and  $W_c$  are the weight matrices, while  $b_i, b_f, b_o$ , and  $b_c$  are the biased terms. These LSTM layers processed the input sequences, learning the temporal dependencies between the biomechanical movements and the Mel-spectrogram features.

- 3) Fully Connected Layer and SoftMax Classification: After processing the sequences through the LSTM layers, the output was passed to a fully connected (dense) layer. This dense layer aggregated the learned features from the LSTM layers, refining the representation of the data:

$$z = W_{\text{dense}} \times h + b_{\text{dense}} \quad (10)$$

where  $W_{\text{dense}}$  and  $b_{\text{dense}}$  are the weights and biases of the dense layer, and ' $h$ ' is the final hidden state from the LSTM layers. The dense layer's output ' $z$ ' was then fed into a softmax activation function to produce a probability distribution over the classes:

$$\hat{y}_i = \frac{e^{z_i}}{\sum_j e^{z_j}} \quad (11)$$

where  $\hat{y}_i$  is the predicted probability for class ' $i$ '. The SoftMax function ensured that the output values were summed to 1, making them interpretable as probabilities for the different musical styles and emotional states.

- 4) Model Training: The model was trained using the categorical cross-entropy loss function, which measured the discrepancy between the predicted class probabilities and the true labels:

$$L = - \sum_{i=1}^N y_i \log(\hat{y}_i) \quad (12)$$

where  $y_i$  is the true label and  $\hat{y}_i$  is the predicted probability for each class. The model's parameters, including the weights of the LSTM and dense layers, were updated using Backpropagation Through Time (BPTT) to minimize this loss. The training process involved updating the model weights to improve its ability to classify the input sequences accurately.

The final output layer provided a probability distribution over the classes, allowing the model to classify each input sequence into one of the predefined categories representing musical styles and emotions (Algorithm 1). By leveraging the sequential nature of biomechanical and Mel-spectrogram data, the LSTM model could recognize complex patterns that feature different expressive nuances in violin performances.

---

**Algorithm 1** Mel-spectrogram-based LSTM model
 

---

**1: Input:**2: **Biomechanical Data:**  $X = \{x_1, x_2, \dots, x_T\}$  where  $x_t$  is the biomechanical feature vector at time  $t$ .3: **Mel-Spectrogram Data:**  $M = \{m_1, m_2, \dots, m_T\}$  where  $m_t$  is the Mel-spectrogram frame at time  $t$ .4: **Number of Epochs:**  $E$ 5: **Learning Rate:**  $\alpha$ **6: Output:**

7: Predicted class probabilities for musical styles and emotions.

**8: Steps:****9: Data Preprocessing:**10: 1.1. Clean and normalize biomechanical data  $X$  to obtain features like joint angles, segmental velocities, and forces.11: 1.2. Convert audio recordings into Mel-spectrograms  $M$  using STFT and Mel filter banks.13: 1.3. Synchronize biomechanical data  $X$  and Mel-spectrogram data  $M$  into sequences:  $D = \{(x_1, m_1), (x_2, m_2), \dots, (x_T, m_T)\}$ 

14: 1.4. Normalize and segment the data into fixed-size windows.

**15: Initialize LSTM Model Parameters:**16: 2.1. Randomly initialize weights  $W_i, W_f, W_o, W_c$  and biases  $b_i, b_f, b_o, b_c$  for LSTM layers.17: 2.2. Initialize weights  $W_{\text{dense}}$  and biases  $b_{\text{dense}}$  for the fully connected layer.**18: Training Phase:**19: **For** epoch in 1 to:20: 3.1. **For Each** training sequence  $D_n = \{(x_1, m_1), \dots, (x_T, m_T)\}$ :21: 3.2. Initialize LSTM cell state  $c_0$  and hidden state  $h_0$ .22: **For**  $t = 1$  to:23: **Compute LSTM Gates:**

$$i_t = \sigma(W_i \times [h_{t-1}, x_t, m_t] + b_i)$$

$$f_t = \sigma(W_f \times [h_{t-1}, x_t, m_t] + b_f)$$

$$o_t = \sigma(W_o \times [h_{t-1}, x_t, m_t] + b_o)$$

24: **Update cell state  $c_t$ :**

$$\tilde{c}_t = \tanh(W_c \times [h_{t-1}, x_t, m_t] + b_c)$$

$$c_t = f_t \times c_{t-1} + i_t \cdot \tilde{c}_t$$

25: **Update hidden state  $h_t$ :**

$$h_t = o_t \times \tanh(c_t)$$

**26: End For**27: 3.3. Obtain final hidden state  $h_T$  and pass it to the fully connected layer:  $z = W_{\text{dense}} \times h_T + b_{\text{dense}}$ 28: 3.4. Apply SoftMax to obtain class probabilities:  $\hat{y}_i = \frac{e^{z_i}}{\sum_j e^{z_j}}$ 29: 3.5. Compute loss  $L$  using categorical cross-entropy:  $L = -\sum_{i=1}^N y_i \log(\hat{y}_i)$ 

30: 3.6. Backpropagate the error through the LSTM and fully connected layers using BPTT to compute gradients.

31: 3.7. Update weights and biases using gradient descent:  $\theta = \theta - \alpha \times \nabla L$ **32: 3.8. End For****33: Prediction Phase:**34: 4.1. For a new input sequence  $D_{\text{test}}$ , compute the class probabilities using the trained LSTM model following steps 3.1 to 3.4.

35: 4.2. Assign the class with the highest probability as the predicted label for musical style or emotion.

**36: End Algorithm**


---

## 3. Results

### 3.1. Descriptive statistics



The descriptive statistics for the kinematic data, as shown in **Table 2** and **Figure 2**, indicate a mean shoulder joint angle of 47° with a Standard Deviation (SD) of 12°, ranging from 26° to 67°. The elbow joint angle averaged 72° with an 11° SD, spanning 51° to 89°, while the wrist joint angle had a mean of 23° with an 8° deviation, ranging from 11° to 39°. Bowing velocity showed a mean of 0.74 m/s, with a SD of 0.21 m/s, and varied between 0.32 m/s and 1.18 m/s. The bowing trajectory deviation averaged 7° with a 4° SD, with a range from 2° to 11°. For the kinetic data, the ground reaction force had a mean of 347.6 N and an SD of 64.9 N, ranging from 251.3 N to 468.7 N. The arm force averaged 13.1 N with a 3.3 N SD, from 7.2 N to 18.9 N. Hand force showed a mean of 7.1 N with a 2.3 N-SD, ranging from 3.4 N to 10.7 N. Regarding acoustic data, the sound intensity had a mean of 74.8 dB and an SD of 5.4 dB, with values ranging from 66.1 dB to 87.6 dB. Vibrato frequency averaged 5.7 Hz with a 0.7 Hz deviation from 4.3 Hz to 6.9 Hz. Vibrato amplitude had a mean of 2.9 mm with a 1.2 mm deviation, ranging from 1.1 mm to 4.4 mm. Articulation clarity, measured on a scale of 1 to 5, averaged 4.1 with an SD of 0.6, ranging from 3.1 to 4.9.

**Table 2.** Results for the descriptive statistics.

Parameter	Mean	Standard deviation	Minimum	Maximum
<b>Kinematic data</b>				
Shoulder joint angle (°)	47	12	26	67
Elbow joint angle (°)	72	11	51	89
Wrist joint angle (°)	23	8	11	39
Bowing velocity (m/s)	0.74	0.21	0.32	1.18
Bowing trajectory deviation (°)	7	4	2	11
<b>Kinetic data</b>				
Ground reaction force (n)	347.6	64.9	251.3	468.7
Arm force (n)	13.1	3.3	7.2	18.9
Hand force (N)	7.1	2.3	3.4	10.7
<b>Acoustic data</b>				
Sound intensity (dB)	74.8	5.4	66.1	87.6
Vibrato frequency (Hz)	5.7	0.7	4.3	6.9
Vibrato amplitude (mm)	2.9	1.2	1.1	4.4
Articulation clarity (Scale 1–5)	4.1	0.6	3.1	4.9

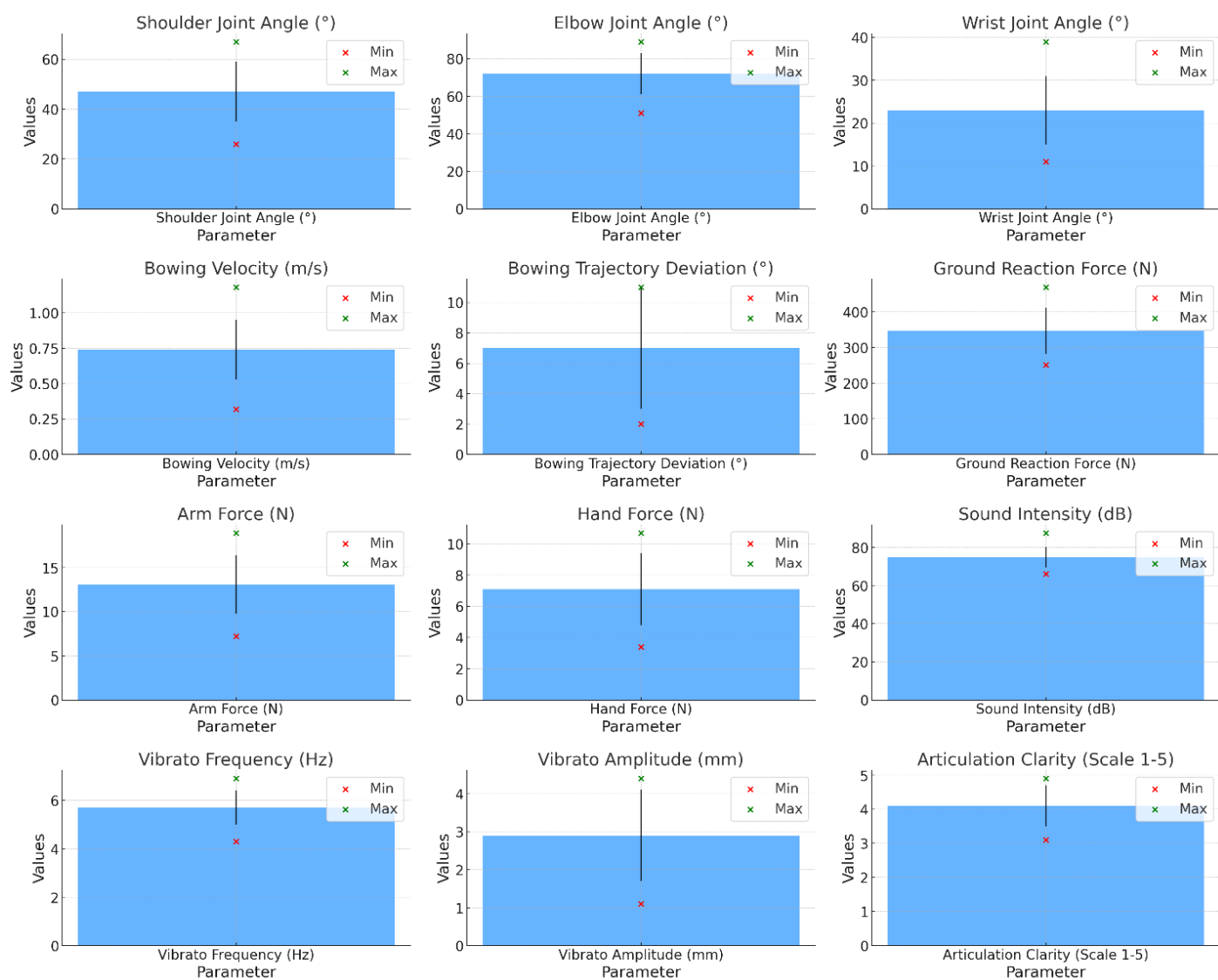


**Figure 2.** Results of description statistics.

### 3.2. Biomechanical analysis

The kinematic findings across different musical styles and emotional contexts are displayed in **Table 3** and **Figure 3**, which show that the shoulder joint angle had a mean of  $44^{\circ}$  (SD:  $10^{\circ}$ ) in “Calm” performances, ranging from  $28^{\circ}$  to  $61^{\circ}$ , while in “Energetic” performances, it averaged  $53^{\circ}$  (SD:  $14^{\circ}$ ) with a range of  $35^{\circ}$  to  $72^{\circ}$ . In “Joyful” contexts, the mean was  $48^{\circ}$  (SD:  $12^{\circ}$ ) with a range from  $32^{\circ}$  to  $65^{\circ}$ , and in “Melancholic” contexts, the mean was  $42^{\circ}$  (SD:  $9^{\circ}$ ) with a range of  $27^{\circ}$  to  $55^{\circ}$ . The elbow joint angle showed a mean of  $70^{\circ}$  (SD:  $8^{\circ}$ ) for “Calm,” with a range from  $55^{\circ}$  to  $83^{\circ}$ , while “Energetic” performances had a higher mean of  $76^{\circ}$  (SD:  $10^{\circ}$ ) ranging from  $58^{\circ}$  to  $89^{\circ}$ . In “Joyful” contexts, the mean was  $74^{\circ}$  (SD:  $9^{\circ}$ ) with a range from  $57^{\circ}$  to  $88^{\circ}$ , and “Melancholic” had the lowest mean at  $68^{\circ}$  (SD:  $7^{\circ}$ ), ranging from  $51^{\circ}$  to  $82^{\circ}$ . Wrist joint angle in “Calm” performances had a mean of  $22^{\circ}$  (SD:  $7^{\circ}$ ), ranging from  $10^{\circ}$  to  $37^{\circ}$ , while in “Energetic” contexts, it averaged  $27^{\circ}$  (SD:  $9^{\circ}$ ) with a range of  $13^{\circ}$  to  $41^{\circ}$ . For “Joyful,” the mean was  $25^{\circ}$  (SD:  $8^{\circ}$ ) with a range of  $12^{\circ}$  to  $39^{\circ}$ , and in “Melancholic,” the mean was  $20^{\circ}$  (SD:  $6^{\circ}$ ) with a range of  $9^{\circ}$  to  $32^{\circ}$ . Bowing velocity had a mean of  $0.61$  m/s (SD:  $0.18$  m/s) for “Calm” performances, ranging

from 0.35 to 0.93 m/s. In “Energetic” contexts, it increased to a mean of 0.89 m/s (SD: 0.24 m/s), ranging from 0.48 to 1.23 m/s. “Joyful” performances showed a mean of 0.78 m/s (SD: 0.21 m/s), ranging from 0.44 to 1.11 m/s, and “Melancholic” had the lowest mean at 0.58 m/s (SD: 0.16 m/s), with a range of 0.30 to 0.82 m/s. Bowing trajectory deviation in “Calm” performances had a mean of 6° (SD: 2°), with a range from 2° to 10°. In “Energetic” contexts, the mean increased to 9° (SD: 3°), ranging from 4° to 14°. “Joyful” performances had a mean of 8° (SD: 3°) with a range of 3° to 12°, while “Melancholic” performances had the lowest mean at 5° (SD: 2°), ranging from 1° to 9°.

**Table 3.** Kinematic findings across different musical styles and emotional contexts.

<b>Kinematic Parameter</b>		<b>Calm</b>	<b>Energetic</b>	<b>Joyful</b>	<b>Melancholic</b>
Shoulder joint angle (°)	Mean:	44	53	48	42
	SD:	10	14	12	9
	Range:	28–61	35–72	32–65	27–55
Elbow joint angle (°)	Mean:	70	76	74	68
	SD:	8	10	9	7
	Range:	55–83	58–89	57–88	51–82
Wrist joint angle (°)	Mean:	22	27	25	20
	SD:	7	9	8	6
	Range:	10–37	13–41	12–39	9–32
Bowing velocity (m/s)	Mean:	0.61	0.89	0.78	0.58
	SD:	0.18	0.24	0.21	0.16
	Range:	0.35–0.93	0.48–1.23	0.44–1.11	0.30–0.82
Bowing trajectory deviation (°)	Mean:	6	9	8	5
	SD:	2	3	3	2
	Range:	2–10	4–14	3–12	1–9

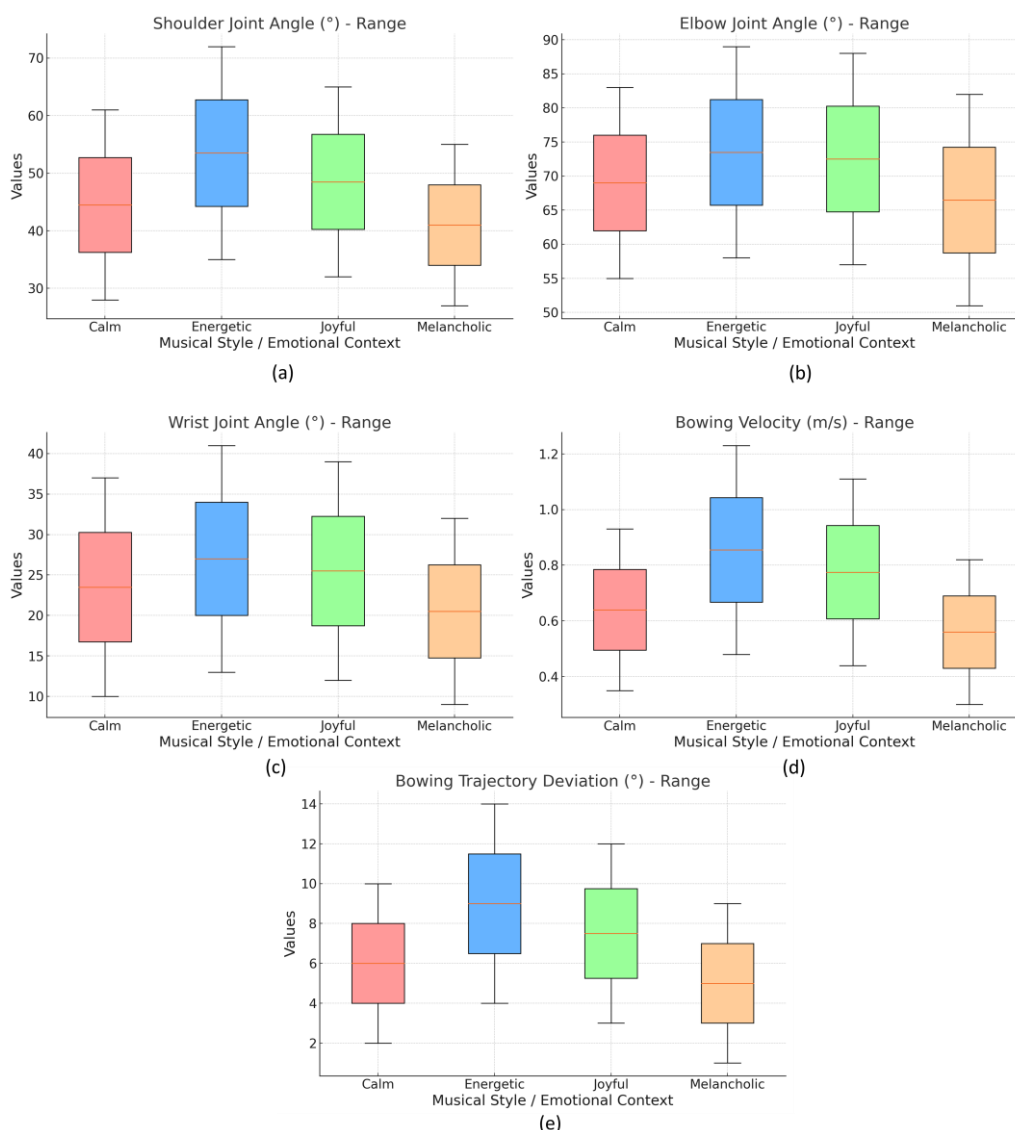


**Figure 3.** Kinematic findings for. **(a)** shoulder joint angle (°); **(b)** elbow joint angle (°); **(c)** wrist joint angle (°); **(d)** bowing velocity (m/s); **(e)** bowing trajectory deviation (°).

### 3.3. Kinetic findings

The kinetic findings across different musical styles and emotional contexts are shown in **Table 4** and **Figure 4**, and they indicate that the ground reaction force in “Calm” performances had a mean of 312 N (SD: 47 N), ranging from 257 N to 416 N. In “Energetic” performances, the mean increased to 368 N (SD: 59 N), ranging from 275 N to 474 N. “Joyful” contexts showed a mean of 342 N (SD: 53 N), with a range of 263 N to 435 N, while “Melancholic” had the lowest mean at 298 N (SD: 44 N), ranging from 240 N to 386 N. Arm force had a mean of 11.2 N (SD: 3.1 N) for “Calm” performances, ranging from 6.5 N to 16.8 N. In “Energetic” contexts, the mean increased to 14.7 N (SD: 3.8 N), ranging from 8.4 N to 19.5 N. “Joyful” performances had a mean of 13.3 N (SD: 3.4 N), ranging from 7.1 N to 17.6 N, while “Melancholic” had the lowest mean arm force at 10.6 N (SD: 2.9 N), with a range of 6.2 N to 15.0 N. Hand force in “Calm” performances had a mean of 5.8 N (SD: 1.7 N), ranging from 3.4 N to 9.2 N. In “Energetic” contexts, the mean was 7.6 N (SD: 2.1 N), ranging from 4.0 N to 10.7 N. “Joyful” performances showed a mean of 6.9 N (SD: 1.9 N), with a

range from 3.8 N to 9.9 N. “Melancholic” had the lowest hand force mean at 5.2 N (SD: 1.6 N), ranging from 3.0 N to 8.3 N. Force plate balance in “Calm” performances had a mean distribution of 48/52% (SD: 3/3%), with a range from 44/56% to 51/49%. In “Energetic” contexts, the mean balance was 45/55% (SD: 4/4%), ranging from 40/60% to 50/50%. The mean balance for “Joyful” performances was 47/53% (SD: 3/3%), ranging from 43/57% to 51/49%. “Melancholic” performances exhibited a balanced mean of 50/50% (SD: 2/2%), ranging from 47/53% to 52/48%.

**Table 4.** The kinetic findings across different musical styles and emotional contexts.

Kinetic Parameter	Calm	Energetic	Joyful	Melancholic
Ground reaction force (N)	Mean: 312	368	342	298
	SD: 47	59	53	44
	Range: 257–416	275–474	263–435	240–386
Arm force (N)	Mean: 11.2	14.7	13.3	10.6
	SD: 3.1	3.8	3.4	2.9
	Range: 6.5–16.8	8.4–19.5	7.1–17.6	6.2–15.0
Hand force (N)	Mean: Mean: 5.8	Mean: 7.6	Mean: 6.9	Mean: 5.2
	SD: SD: 1.7	SD: 2.1	SD: 1.9	SD: 1.6
	Range: 3.4–9.2	4.0–10.7	3.8–9.9	3.0–8.3
Force plate balance (%)	Mean: 48/52	45/55	47/53	50/50
	SD: 3/3	4/4	3/3	2/2
	Range: 44/56–51/49	40/60–50/50	43/57–51/49	47/53–52/48

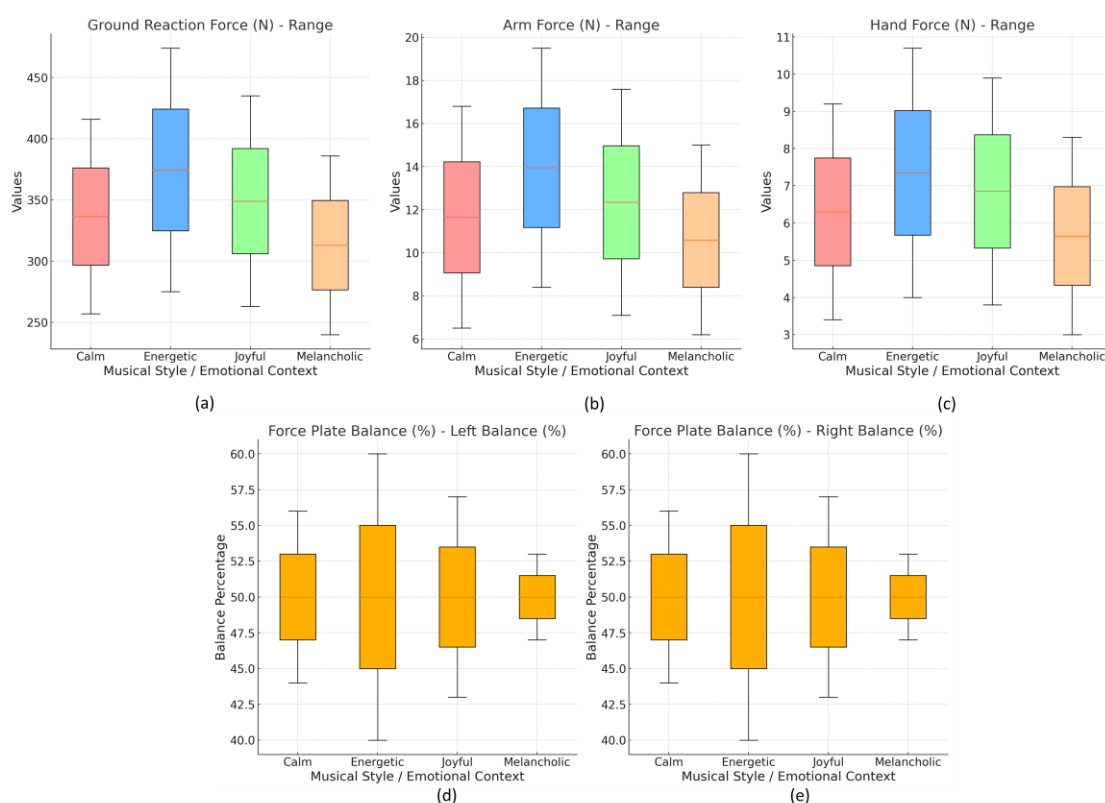


**Figure 4.** Kinetic findings for. (a) ground reaction force (N); (b) arm force (N); (c) hand force (N); (d) force plate balance (%) for left balance; (e) force plate balance (%) for right balance.

### 3.4. Correlation with audio features

The correlations between key biomechanical parameters and acoustic features are shown in **Table 5** and **Figure 5**, which reveal that shoulder joint angle had a moderate positive correlation with sound intensity across all contexts, being strongest in “Energetic” (0.68) and weakest in “Melancholic” (0.38). The correlation between shoulder joint angle and vibrato amplitude was also highest in “Energetic” (0.60) and lowest in “Melancholic” (0.30). The elbow joint angle showed a moderate correlation with sound intensity, peaking in “Energetic” (0.63) and lowest in “Melancholic” (0.35). Its correlation with vibrato frequency was highest in “Energetic” (0.58) and lowest in “Melancholic” (0.32). Bowing velocity exhibited a strong correlation with sound intensity, particularly in “Energetic” (0.75) and a moderate one in “Melancholic” (0.50). Its correlation with articulation clarity was highest in “Energetic” (0.70) and lowest in “Melancholic” (0.46). Ground reaction force showed a moderate correlation with sound intensity, being highest in “Energetic” (0.57) and lowest in “Melancholic” (0.33). Arm force had a moderate to strong correlation with vibrato amplitude, most vital in “Energetic” (0.65) and weakest in “Melancholic” (0.37). Its correlation with sound intensity was highest in “Energetic” (0.69) and lowest in “Melancholic” (0.39). Hand force had a moderate correlation with articulation clarity, peaking in “Energetic” (0.63) and lowest in “Melancholic” (0.40).

**Table 5.** The correlations between key biomechanical (kinematic and kinetic) parameters and acoustic features across different musical styles and emotional contexts.

Biomechanical parameter	Acoustic feature	Calm	Energetic	Joyful	Melancholic
Shoulder joint angle (°)	Sound intensity (dB)	0.45	0.68	0.52	0.38
	Vibrato amplitude (mm)	0.34	0.60	0.41	0.30
Elbow joint angle (°)	Sound intensity (dB)	0.40	0.63	0.48	0.35
	Vibrato frequency (Hz)	0.37	0.58	0.44	0.32
Bowing velocity (m/s)	Sound intensity (dB)	0.56	0.75	0.62	0.50
	Articulation clarity	0.48	0.70	0.55	0.46
Ground reaction force (N)	Sound intensity (dB)	0.38	0.57	0.49	0.33
Arm force (N)	Vibrato amplitude (mm)	0.42	0.65	0.50	0.37
	Sound intensity (dB)	0.44	0.69	0.54	0.39
Hand force (N)	Articulation clarity	0.46	0.63	0.51	0.40

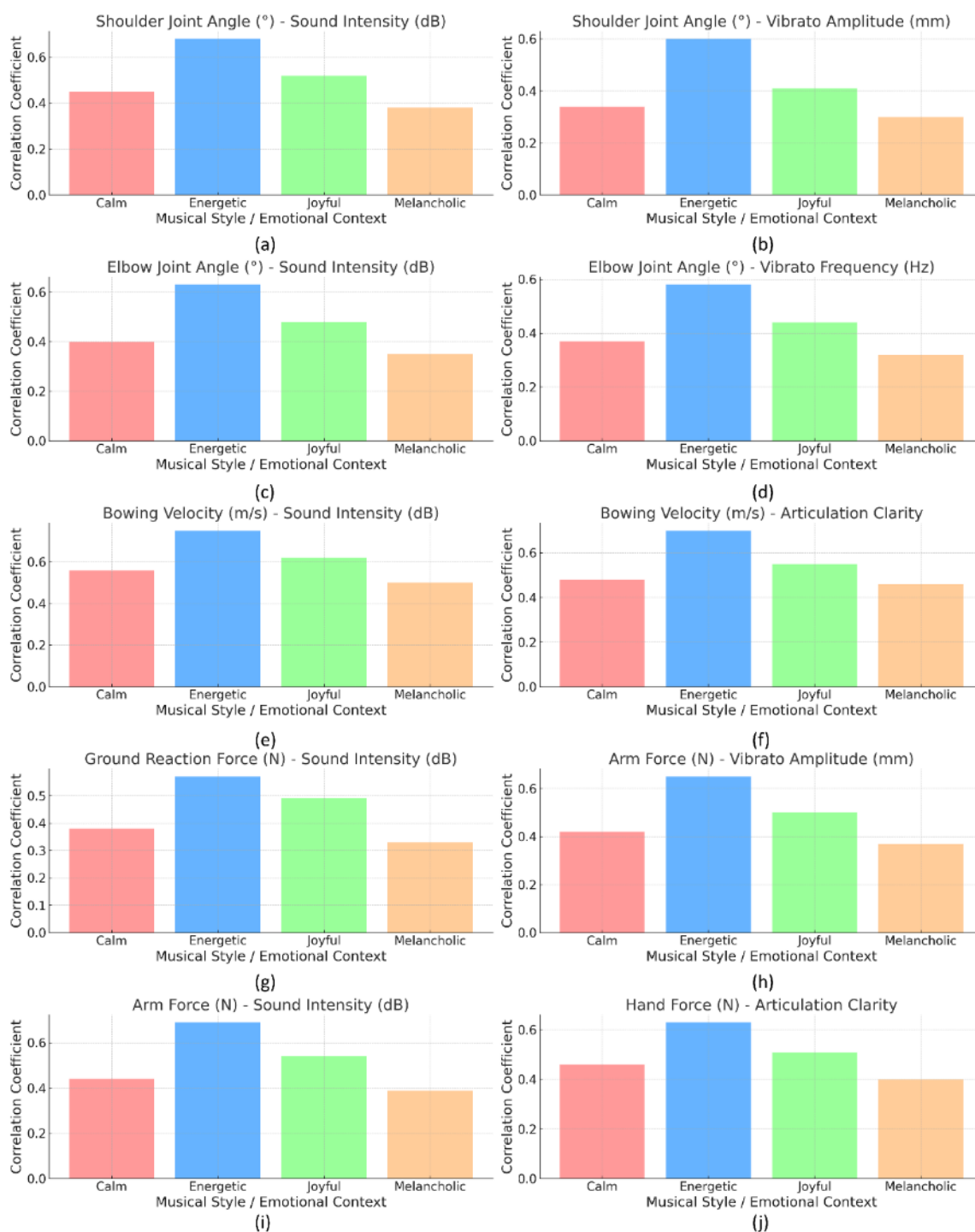


**Figure 5.** Correlations between. (a) shoulder joint angle (°)—sound intensity (dB); (b) shoulder joint angle (°)—vibrato amplitude (mm); (c) elbow joint angle (°)—sound intensity (dB); (d) elbow joint angle (°)—vibrato frequency (Hz); (e) bowing velocity (m/s)—and intensity (dB); (f) bowing velocity (m/s)—articulation clarity; (g) ground reaction force (N)—sound intensity (dB); (h) arm force (N)—vibrato amplitude (mm); (i) arm force (N)—sound intensity (dB); (j) hand force (N)—articulation clarity.

### 3.5. Audio analysis

The Mel-spectrogram features across different musical styles and emotional contexts are shown in **Table 6** and **Figure 6**, and they indicate that peak frequency was highest in “Energetic” performances with a mean of 947 Hz (SD: 113 Hz), ranging

from 779 Hz to 1103 Hz, and lowest in “Melancholic” with a mean of 553 Hz (SD: 68 Hz), ranging from 423 Hz to 668 Hz. In “Calm” and “Joyful” contexts, the means were 603 Hz (SD: 77 Hz) and 807 Hz (SD: 92 Hz), respectively. The spectral centroid, representing the “brightness” of the sound, was highest in “Energetic” performances with a mean of 1093 Hz (SD: 117 Hz), ranging from 903 Hz to 1253 Hz, and lowest in “Melancholic” at 647 Hz (SD: 71 Hz), with a range from 523 Hz to 779 Hz. “Calm” and “Joyful” had means of 703 Hz (SD: 82 Hz) and 953 Hz (SD: 98 Hz), respectively. Spectral bandwidth, indicating the range of frequencies, was broadest in “Energetic” with a mean of 273 Hz (SD: 41 Hz), ranging from 203 Hz to 319 Hz, and narrowest in “Melancholic” with a mean of 163 Hz (SD: 24 Hz), ranging from 121 Hz to 199 Hz. In “Calm” and “Joyful,” the means were 183 Hz (SD: 31 Hz) and 227 Hz (SD: 36 Hz), respectively. Spectral contrast was highest in “Energetic” performances with a mean of 31 dB (SD: 6 dB), ranging from 25 dB to 37 dB, and lowest in “Melancholic” at 21 dB (SD: 2 dB), ranging from 17 dB to 27 dB. “Calm” and “Joyful” had means of 23 dB (SD: 3 dB) and 27 dB (SD: 4 dB), respectively. Spectral flatness, which indicates the noisiness of the sound, was highest in “Melancholic” with a mean of 0.34 (SD: 0.02), ranging from 0.31 to 0.39, and lowest in “Energetic” with a mean of 0.22 (SD: 0.03), ranging from 0.17 to 0.28. “Calm” and “Joyful” had means of 0.33 (SD: 0.04) and 0.27 (SD: 0.05), respectively. The zero-crossing rate, indicating the rate of signal changes, was highest in “Energetic” with a mean of 0.13 (SD: 0.03), ranging from 0.09 to 0.15, and lowest in “Melancholic” with a mean of 0.06 (SD: 0.01), ranging from 0.05 to 0.08. “Calm” and “Joyful” contexts had means of 0.09 (SD: 0.02) and 0.11 (SD: 0.02), respectively.

**Table 6.** Mel-spectrogram features across different musical styles and emotional contexts.

Mel-Spectrogram Feature		Calm	Energetic	Joyful	Melancholic
Peak Frequency (Hz)	Mean:	603	947	807	553
	SD:	77	113	92	68
	Range:	482–719	779–1103	654–963	423–668
Spectral Centroid (Hz)	Mean:	703	1093	953	647
	SD:	82	117	98	71
	Range:	552–849	903–1253	751–1103	523–779
Spectral Bandwidth (Hz)	Mean:	183	273	227	163
	SD:	31	41	36	24
	Range:	131–229	203–319	181–279	121–199
Spectral Contrast (dB)	Mean:	23	31	27	21
	SD:	3	6	4	2
	Range:	18–29	25–37	23–33	17–27
Spectral Flatness	Mean:	0.33	0.22	0.27	0.34
	SD:	0.04	0.03	0.05	0.02
	Range:	0.26–0.39	0.17–0.28	0.21–0.33	0.31–0.39
Zero-Crossing Rate	Mean:	0.09	0.13	0.11	0.06
	SD:	0.02	0.03	0.02	0.01
	Range:	0.06–0.10	0.09–0.15	0.08–0.13	0.05–0.08



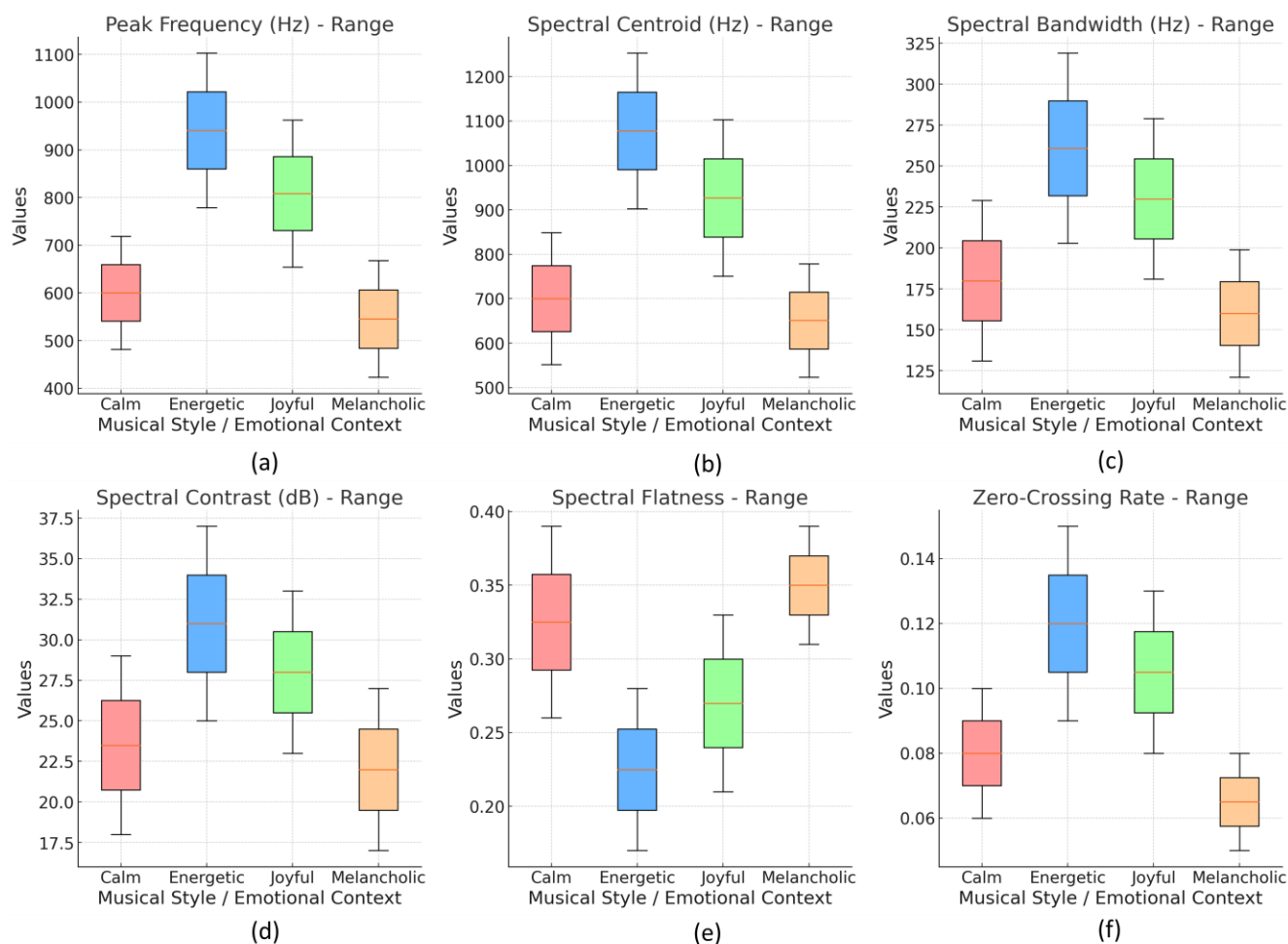


**Figure 6.** Mel-spectrogram attribute for. **(a)** Peak Frequency (Hz); **(b)** spectral centroid (Hz); **(c)** spectral bandwidth (Hz); **(d)** spectral contrast (dB); **(e)** spectral flatness; **(f)** zero-crossing rate.

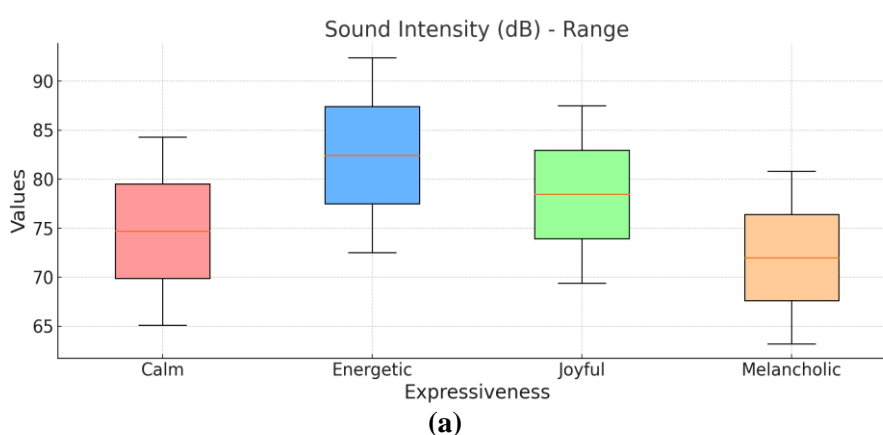
### 3.6. Sound and expressiveness

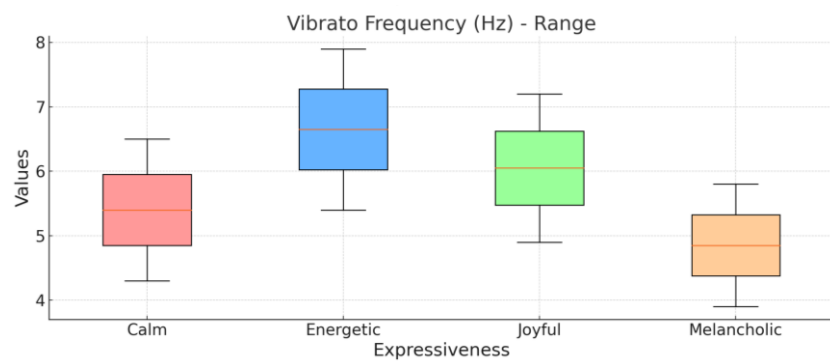
The sound features and their association with expressive elements across different musical styles and emotional contexts are depicted in **Table 7** and **Figure 7**, which reveal that sound intensity was highest in “Energetic” performances with a mean of 83.7 dB (SD: 6.3 dB), ranging from 72.5 dB to 92.4 dB, and lowest in “Melancholic” with a mean of 71.9 dB (SD: 4.9 dB), ranging from 63.2 dB to 80.8 dB. In “Calm” and “Joyful” contexts, the means were 74.2 dB (SD: 5.2 dB) and 78.6 dB (SD: 5.7 dB), respectively. Vibrato frequency, indicating the rate of pitch variation, was highest in “Energetic” performances with a mean of 6.8 Hz (SD: 0.9 Hz), ranging from 5.4 Hz to 7.9 Hz, and lowest in “Melancholic” with a mean of 4.8 Hz (SD: 0.6 Hz), ranging from 3.9 Hz to 5.8 Hz. “Calm” and “Joyful” had means of 5.4 Hz (SD: 0.7 Hz) and 6.1 Hz (SD: 0.8 Hz), respectively. Vibrato amplitude, reflecting the extent of pitch variation, was widest in “Energetic” performances with a mean of 3.4 mm (SD: 1.3 mm), ranging from 2.0 mm to 5.6 mm, and narrowest in “Melancholic” with a mean of 2.3 mm (SD: 0.8 mm), ranging from 1.0 mm to 3.6 mm. “Calm” and “Joyful” contexts had means of 2.7 mm (SD: 1.0 mm) and 3.1 mm (SD: 1.1 mm), respectively. Articulation clarity, measured on a scale of 1 to 5, was highest in “Energetic” performances with a mean of 4.6 (SD: 0.5), ranging from 4.0 to 5.0, and

lowest in “Melancholic” with a mean of 3.9 (SD: 0.5), ranging from 3.0 to 4.8. “Calm” and “Joyful” had means of 4.1 (SD: 0.6) and 4.4 (SD: 0.7), respectively. Dynamic range, indicating the difference between the loudest and softest sounds, was most significant in “Energetic” performances with a mean of 24.9 dB (SD: 4.5 dB), ranging from 19.0 dB to 29.8 dB, and most minor in “Melancholic” with a mean of 17.3 dB (SD: 3.2 dB), ranging from 13.1 dB to 22.6 dB. “Calm” and “Joyful” contexts had means of 18.4 dB (SD: 3.7 dB) and 21.7 dB (SD: 4.0 dB), respectively.

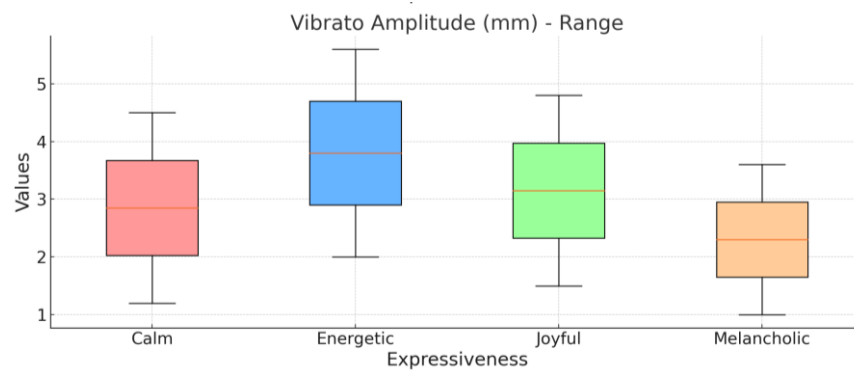
**Table 7.** Sound features and their association with expressive elements across different musical styles and emotional contexts.

Sound characteristic		Calm	Energetic	Joyful	Melancholic
Sound intensity (dB)	Mean:	74.2	83.7	78.6	71.9
	SD:	5.2	6.3	5.7	4.9
	Range:	65.1–84.3	72.5–92.4	69.4–87.5	63.2–80.8
Vibrato frequency (Hz)	Mean:	5.4	6.8	6.1	4.8
	SD:	0.7	0.9	0.8	0.6
	Range:	4.3–6.5	5.4–7.9	4.9–7.2	3.9–5.8
Vibrato amplitude (mm)	Mean:	2.7	3.4	3.1	2.3
	SD:	1.0	1.3	1.1	0.8
	Range:	1.2–4.5	2.0–5.6	1.5–4.8	1.0–3.6
Articulation clarity	Mean:	4.1 (scale 1–5)	4.6 (scale 1–5)	4.4 (scale 1–5)	3.9 (scale 1–5)
	SD:	0.6	0.5	0.7	0.5
	Range:	3.2–4.9	4.0–5.0	3.3–5.0	3.0–4.8
Dynamic range (dB)	Mean:	18.4	24.9	21.7	17.3
	SD:	3.7	4.5	4.0	3.2
	Range:	12.5–24.7	19.0–29.8	15.6–26.4	13.1–22.6

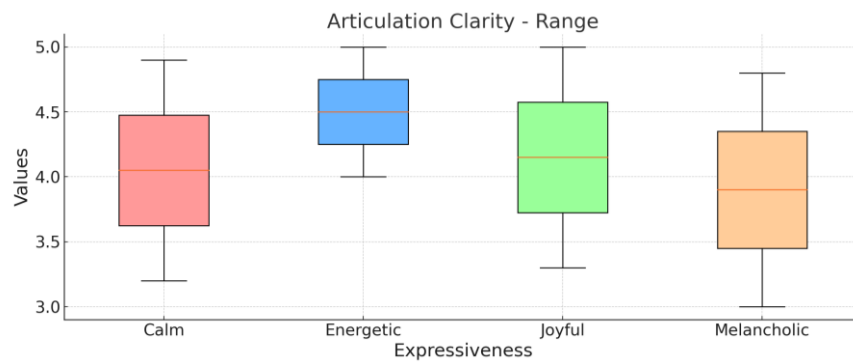




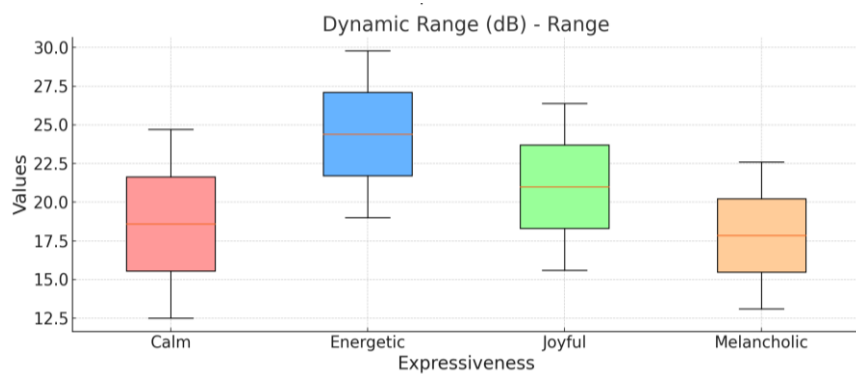
(b)



(c)



(d)



(e)

**Figure 7.** Sound characteristics and their association with. (a) sound intensity (dB); (b) vibrato frequency (Hz); (c) vibrato amplitude (mm); (d) articulation clarity; (e) dynamic range (dB).

### 3.7. ML model performance

As displayed in **Table 8** and **Figure 8**, during the ML model's training and validation process, the key performance metrics show a steady decrease in training and validation loss over the epochs, with training loss starting at 1.203 in epoch 1 and reducing to 0.277 by epoch 100. Validation loss followed a similar trend, decreasing from 1.315 to 0.459 over the same period. Training accuracy increased consistently from 58.4% at epoch 1 to 96.5% at epoch 100, while validation accuracy improved from 54.3% to 92.5%. Precision started at 55.6% in epoch 1 and rose to 94.3% by epoch 100. Recall followed a similar pattern, beginning at 53.7% and reaching 92.6%. The F1-score, reflecting the harmonic mean of precision and recall, improved from 54.6% at the start of training to 93.4% at epoch 100. These metrics indicate a consistent improvement in the model's ability to accurately identify musical styles and emotions, with both training and validation metrics stabilizing in the latter epochs, suggesting effective learning and generalization.

**Table 8.** Performance metrics during the ML model's training and validation process.

Epoch	Training loss	Validation loss	Training accuracy (%)	Validation accuracy (%)	Precision (%)	Recall (%)	F1-score (%)
1	1.203	1.315	58.4	54.3	55.6	53.7	54.6
5	0.854	0.926	72.1	68.9	70.2	67.8	69.0
10	0.672	0.705	81.4	78.3	79.1	77.5	78.3
15	0.551	0.622	86.5	82.7	84.6	81.2	82.9
20	0.497	0.583	88.3	84.6	86.1	83.4	84.7
25	0.459	0.548	89.7	86.1	87.8	85.2	86.5
30	0.430	0.524	90.8	87.5	89.1	86.9	88.0
35	0.410	0.510	91.6	88.2	89.7	87.4	88.5
40	0.391	0.501	92.3	88.7	90.4	88.1	89.2
45	0.376	0.492	92.8	89.1	90.9	88.6	89.7
50	0.362	0.486	93.3	89.6	91.5	89.2	90.3
55	0.349	0.481	93.7	90.1	91.8	89.9	90.8
60	0.337	0.476	94.1	90.4	92.2	90.3	91.2
65	0.327	0.473	94.5	90.8	92.6	90.7	91.6
70	0.318	0.470	94.8	91.0	92.9	91.1	92.0
75	0.310	0.467	95.1	91.3	93.1	91.4	92.3
80	0.302	0.465	95.4	91.6	93.4	91.7	92.5
85	0.295	0.463	95.7	91.8	93.7	91.9	92.8
90	0.288	0.461	96.0	92.1	93.9	92.2	93.0
95	0.282	0.460	96.2	92.3	94.1	92.4	93.2
100	0.277	0.459	96.5	92.5	94.3	92.6	93.4

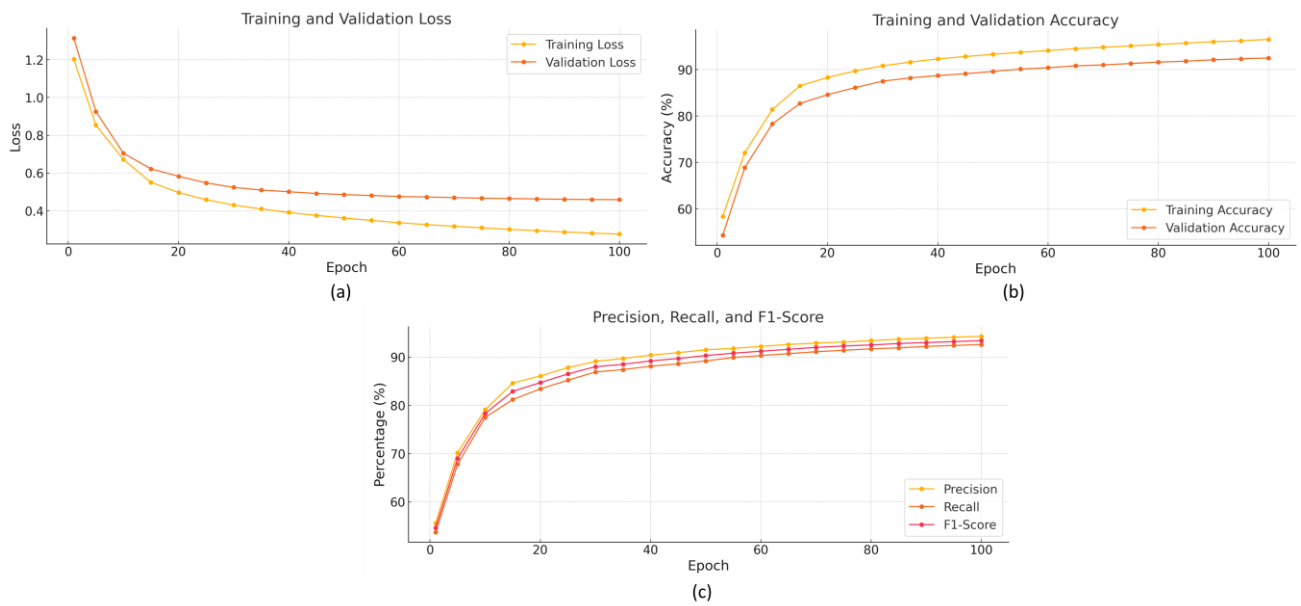


**Figure 8.** Performance of the ML model against. **(a)** training and validation loss; **(b)** training and validation accuracy; **(c)** precision, recall, and F1-score.

#### 4. Conclusion and future work

The findings of this study demonstrate the effectiveness of integrating biomechanical analysis with ML, specifically Mel-spectrogram-based LSTM modeling, to automate the identification of musical styles and emotions in violin performances. By analyzing synchronized biomechanical and acoustic data, the study reveals a strong relationship between a violinist's physical movements and the expressive qualities of their performance. Key biomechanical parameters such as joint angles, bowing velocity, and force dynamics correlate significantly with audio features like sound intensity, vibrato frequency, and articulation clarity, highlighting the nuanced ways musicians convey different styles and emotions. The LSTM model showed high accuracy in classifying musical styles and emotions, achieving a validation accuracy of 92.5%, with precision, recall, and F1-score exceeding 92%. These results indicate that ML can effectively capture the complex temporal patterns linking PM and ME, contributing to a more objective and comprehensive understanding than traditional qualitative methods. This automated approach has significant implications for music analysis, education, and interactive performance systems, providing a framework for real-time feedback and training tools for musicians. Despite the promising outcomes, this study also highlights areas for further exploration. The model's performance, while robust, could be enhanced by incorporating additional features such as emotional context in real-time performance settings.

Future work could extend this framework to other musical instruments and genres, furthering our understanding of the interplay between biomechanics and ME. Overall, this study contributes to bridging the gap between the artistic and scientific perspectives on music performance, demonstrating the potential of combining biomechanics and machine learning to enrich our understanding of violin playing.

**Ethical approval:** Not applicable.

**Conflict of interest:** The author declares no conflict of interest.

## References

1. Kucherenko S, Sediuk I. Aesthetic Experience and Its Expressions in Music Performance. *International Review of the Aesthetics and Sociology of Music*. 2020; 51(1): 19–28.
2. Bedoya D, Arias P, Rachman L, et al. Even violins can cry: specifically vocal emotional behaviours also drive the perception of emotions in non-vocal music. *Philosophical Transactions of the Royal Society B: Biological Sciences*. 2021; 376(1840). doi: 10.1098/rstb.2020.0396
3. Trollmo S. A method-based approach to historical violin playing: performance practice from a contemporary perspective [PhD thesis]. Boston University; 2020.
4. Kim N. Expressivity in the Melodic Line: Developing Musicality in Violin Students [PhD thesis]. The Florida State University; 2020.
5. Meissner H. Theoretical Framework for Facilitating Young Musicians' Learning of Expressive Performance. *Frontiers in Psychology*. 2021; 11: 584171. doi: 10.3389/fpsyg.2020.584171
6. Lerch A, Arthur C, Pati A, Gururani S. An interdisciplinary review of music performance analysis. *Transactions of the International Society for Music Information Retrieval*. 2021; 3(1): 221–245. doi: 10.5334/tismir.53
7. Wolf E, Möller D, Ballenberger N, et al. Marker-Based Method for Analyzing the Three-Dimensional Upper Body Kinematics of Violinists: Reproducibility. *Medical Problems of Performing Artists*. 2022; 37(3): 176–191. doi: 10.21091/mppa.2022.3025
8. Turner C, Visentin P, Oye D, et al. Pursuing Artful Movement Science in Music Performance: Single Subject Motor Analysis with Two Elite Pianists. *Perceptual and Motor Skills*. 2021; 128(3): 1252–1274. doi: 10.1177/00315125211003493
9. Kyriakou T, de la Campa Crespo MÁ, Panayiotou A, et al. Virtual Instrument Performances (VIP): A Comprehensive Review. *Computer Graphics Forum*. 2024; 43(2). doi: 10.1111/cgf.15065
10. Erdem C, Lan Q, Jensenius AR. Exploring relationships between effort, motion, and sound in new musical instruments. *Human Technology*. 2020; 16(3): 310–347.
11. Freire S, Santos G, Armondes A, et al. Evaluation of Inertial Sensor Data by a Comparison with Optical Motion Capture Data of Guitar Strumming Gestures. *Sensors*. 2020; 20(19): 5722. doi: 10.3390/s20195722
12. Jensenius AR. *Sound actions: Conceptualizing musical instruments*. MIT Press; 2022.
13. Sharma, G. (2023). *Audio Texture Analysis of Biomedical Audio Signals* [PhD thesis]. Toronto Metropolitan University; 2023.
14. Gupta C, Li H, Goto M. (2022). Deep learning approaches in topics of singing information processing. *IEEE/ACM Transactions on Audio, Speech, and Language Processing*; 2022. pp. 2422–2451.
15. Alfaras M, Primett W, Umair M, et al. Biosensing and Actuation—Platforms Coupling Body Input-Output Modalities for Affective Technologies. *Sensors*. 2020; 20(21): 5968. doi: 10.3390/s20215968
16. Napier T, Ahn E, Allen-Ankins S, et al. Advancements in preprocessing, detection and classification techniques for ecoacoustic data: A comprehensive review for large-scale Passive Acoustic Monitoring. *Expert Systems with Applications*. 2024; 252: 124220. doi: 10.1016/j.eswa.2024.124220
17. Van Houdt G, Mosquera C, Nápoles G. A review on the long short-term memory model. *Artificial Intelligence Review*. 2020; 53(8): 5929–5955. doi: 10.1007/s10462-020-09838-1
18. Chikkamath S, Nirmala SR. Melody generation using LSTM and BI-LSTM Network. In: *Proceedings of the 2021 International Conference on Computational Intelligence and Computing Applications (ICCICA)*; 2021. pp. 1–6.
19. Sarangi V. *Biological and biomimetic machine learning for automatic classification of human gait* [PhD thesis]. University of York; 2020.
20. Indumathi N et al., Impact of Fireworks Industry Safety Measures and Prevention Management System on Human Error Mitigation Using a Machine Learning Approach, *Sensors*, 2023, 23 (9), 4365; DOI:10.3390/s23094365.
21. Parkavi K et al., Effective Scheduling of Multi-Load Automated Guided Vehicle in Spinning Mill: A Case Study, *IEEE Access*, 2023, DOI:10.1109/ACCESS.2023.3236843.

22. Ran Q et al., English language teaching based on big data analytics in augmentative and alternative communication system, Springer-International Journal of Speech Technology, 2022, DOI:10.1007/s10772-022-09960-1.
23. Ngangbam PS et al., Investigation on characteristics of Monte Carlo model of single electron transistor using Orthodox Theory, Elsevier, Sustainable Energy Technologies and Assessments, Vol. 48, 2021, 101601, DOI:10.1016/j.seta.2021.101601.
24. Huidan Huang et al., Emotional intelligence for board capital on technological innovation performance of high-tech enterprises, Elsevier, Aggression and Violent Behavior, 2021, 101633, DOI:10.1016/j.avb.2021.101633.
25. Sudhakar S, et al., Cost-effective and efficient 3D human model creation and re-identification application for human digital twins, Multimedia Tools and Applications, 2021. DOI:10.1007/s11042-021-10842-y.
26. Prabhakaran N et al., Novel Collision Detection and Avoidance System for Mid-vehicle Using Offset-Based Curvilinear Motion. Wireless Personal Communication, 2021. DOI:10.1007/s11277-021-08333-2.
27. Balajee A et al., Modeling and multi-class classification of vibroarthrographic signals via time domain curvilinear divergence random forest, J Ambient Intell Human Comput, 2021, DOI:10.1007/s12652-020-02869-0.
28. Omnia SN et al., An educational tool for enhanced mobile e-Learning for technical higher education using mobile devices for augmented reality, Microprocessors and Microsystems, 83, 2021, 104030, DOI:10.1016/j.micpro.2021.104030 .
29. Firas TA et al., Strategizing Low-Carbon Urban Planning through Environmental Impact Assessment by Artificial Intelligence-Driven Carbon Foot Print Forecasting, Journal of Machine and Computing, 4(4), 2024, doi: 10.53759/7669/jmc202404105.
30. Shaymaa HN, et al., Genetic Algorithms for Optimized Selection of Biodegradable Polymers in Sustainable Manufacturing Processes, Journal of Machine and Computing, 4(3), 563-574, <https://doi.org/10.53759/7669/jmc202404054>.
31. Hayder MAG et al., An open-source MP + CNN + BiLSTM model-based hybrid model for recognizing sign language on smartphones. Int J Syst Assur Eng Manag (2024). <https://doi.org/10.1007/s13198-024-02376-x>
32. Bhavana Raj K et al., Equipment Planning for an Automated Production Line Using a Cloud System, Innovations in Computer Science and Engineering. ICICSE 2022. Lecture Notes in Networks and Systems, 565, 707–717, Springer, Singapore. DOI:10.1007/978-981-19-7455-7\_57.